JCTC Journal of Chemical Theory and Computation

Article

pubs.acs.org/JCTC

Influence of the Density Functional and Basis Set on the Relative Stabilities of Oxygenated Isomers of Diiron Models for the Active Site of [FeFe]-Hydrogenase

Caiping Liu,[†,‡] Tianbiao Liu,[†,§] and Michael B. Hall*[,†]

[†]Department of Chemistry, Texas A&M University, College Station, Texas 77843-3255, United States

[‡]State Key Laboratory of Structure Chemistry, Fujian Institute of Research on the Structure of Matter, Chinese Academy of Sciences, Fuzhou, Fujian, P. R. China, 350002

[§]Energy Processes and Materials Division, Pacific Northwest National Laboratory, 902 Battelle Boulevard, P.O. Box 999, Richland, Washington 99352, United States

Supporting Information

ABSTRACT: A series of different density functional theory (DFT) methodologies (24 functionals) in conjunction with a variety of six different basis sets (BSs) was employed to investigate the relative stabilities in the oxygenated isomers of diiron complexes that mimic the active site of [FeFe]-hydrogenase: (μ-pdt)[Fe(CO)$_2$L][Fe(CO)$_2$L′] (pdt = propane-1,3-dithiolate; L = L′ = CO (**1**); L = PPh$_3$, L′ = CO (**2**); L = PMe$_3$, L′ = CO (**3**); L = L′ = PMe$_3$ (**4**). Although the enzyme may have a variety of possible sites for oxygenation, the model complexes would necessarily be oxygenated at either the diiron bridging site (***μ*-O**) or at a sulfur (**SO**). Previous DFT studies with both B3LYP and TPSS functionals predicted a more stable ***μ*-O** isomer, whereas only the **SO** isomer was observed experimentally (*J. Am. Chem. Soc.* **2009**, 131, 8296−8307). Here, further calculations reveal that the relative stabilities of the **SO** and ***μ*-O** isomers are extremely sensitive to the choice of the functional, moderately sensitive to the S basis set, but not to the Fe basis set. The relative free energies [G_{solv}(***μ*-O**) − G_{solv}(**SO**)] range from +10 to −60 kcal/mol, a range much larger than what would have been expected on the basis of the previous DFT results. Benchmarking of these results against coupled cluster with single and double excitation calculations, which predict that the **SO** isomer is favored, shows that the best performing functionals are BP86 and PBE0, while B97-D, M05, and SVWN overestimate and B2PLYP, BH&HLYP, BMK, M06-HF, and M06-2X underestimate the energy differences. Most of the variation occurs with the ***μ*-O** isomer and appears to be associated with a functional's ability to predict the strength of the Fe−Fe bond in the reactant. With respect to the S basis set, it appears that the S═O bond is sensitive to the nature of the d polarization functions available on the S atom. The S seems to need a d function more diffuse than the d orbital optimized to provide polarization for the S atom alone; that is, S seems to need a d orbital that has strong overlap with the O atom's valence 2p. Other basis functions and the relative position of the PR$_3$ (R = Ph and Me) substituent groups have smaller influences on the free energy differences.

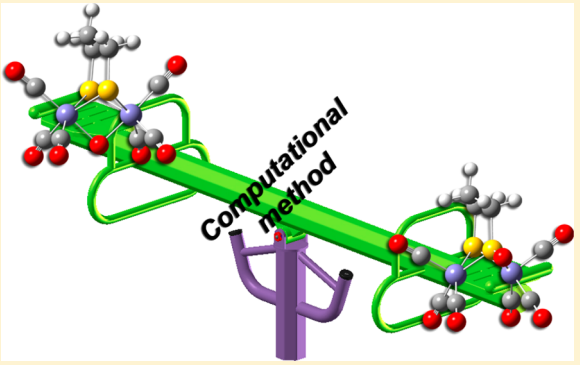

I. INTRODUCTION

Since [FeFe]-hydrogenase and [NiFe]-hydrogenase catalyze the reduction of protons (mainly the former) and oxidation of dihydrogen (mainly the latter) at pH = 7, they have been touted as promising leads for alternatives to platinum electrodes for electrochemical hydrogen cells, and considerable effort has been devoted to their studies.[1−5] Problematically, these hydrogenases are inactivated by O_2.[6−9] [NiFe]-hydrogenase can be reactivated by reduction, while the deleterious effect of O_2 on most [FeFe]-hydrogenases appears irreversible. Thus, the high sensitivity of [FeFe]-hydrogenase to O_2 becomes an obstacle to the development of synthetic catalytic materials. As noted by Farmer and Grapperhaus et al., the nucleophilicity of the bridging sulfur might be utilized as a possible moderator to limit and repair the O_2-damaged hydrogenase, especially in the sulfur-rich [NiFe]-hydrogenase.[10,11]

Recent work reported the mechanism for oxygen damage and repair processes at the diiron subsite of the [FeFe]-hydrogenase active site in a series of diiron dithiolate complexes, (μ-pdt)[Fe(CO)$_2$L][Fe(CO)$_2$L′] (pdt = propane-1,3-dithiolate; L = L′ = CO (**1**); L = PPh$_3$, L′ = CO (**2**); L = PMe$_3$, L′ = CO (**3**); L = L′ = PMe$_3$ (**4**).[12] In these experiments, *m*-chloroperoxybenzoic acid (*m*-CPBA) and dimethyldioxirane (DDO) were utilized as the O atom donors. Although diiron μ-

Received: July 10, 2014

   dx.doi.org/10.1021/ct500594z | J. Chem. Theory Comput. XXXX, XXX, XXX−XXX

Scheme 1. Models Studied in This Investigation

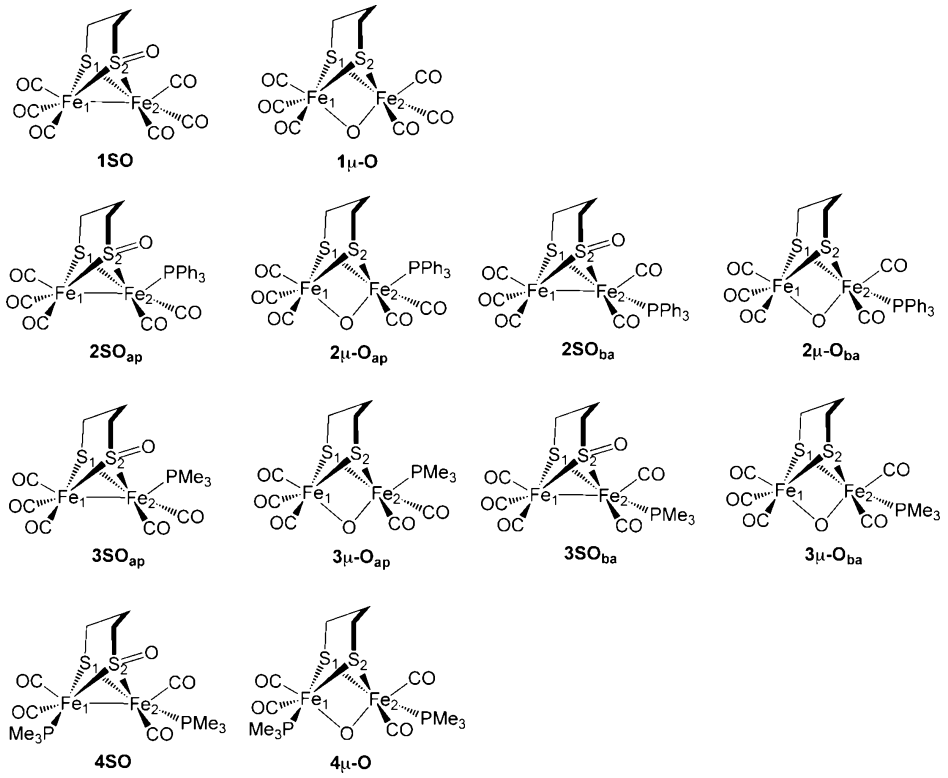

oxo (μ-**O**) complexes are common products in diiron chemistry,[13,14] only the sulfur−oxygenated species (**SO**) were generated (see Scheme 1).[12] In contrast, density functional theory (DFT) calculations predicted that the μ-**O** isomers were thermodynamically favored with both B3LYP and TPSS functionals.[12]

Although DFT with the exact exchange-correlation functional and a complete one-electron basis set would give the exact Kohn−Sham ground-state energy, it has been well-documented that different functionals can lead to different predictions, especially for the relative energies of the transition metal systems.[15−27] For instance, in studies of the mechanism of the Grubbs catalysts, M06 was the best performing, as judged by the energies of the reaction mechanism, among 39 examined DFT functionals, while the popular B3LYP functional performed poorly.[16]

As a prelude to a study of the mechanism of the oxygenation reactions of the hydrogenases, we have re-examined the relative energies of the μ-**O** and **SO** isomers by a wide range of DFT functionals and basis sets. To our surprise, we discovered that these energies were much more sensitive to the functionals than appeared to be the case from the initial work. Twenty-four DFT functionals in combination with six basis sets were employed. In addition, coupled cluster with single and double excitations (CCSD) calculations were carried out to assess the performance of DFT functionals for the smallest **1SO** and **1**μ-**O** models. The computational methods and calculated results will be described and discussed in detail in Sections II and III, respectively.

II. COMPUTATIONAL DETAILS

A. Studied Models. Experimentally, only **1SO**, $\mathbf{2SO}_{ap}$, $\mathbf{3SO}_{ap}$, and **4SO** complexes were synthesized (see Scheme 1), whereas in our investigation, the isomeric structures with the PR_3 (R = Ph and Me) group at the basal site (i.e., $\mathbf{2SO}_{ba}$ and $\mathbf{3SO}_{ba}$, see Scheme 1) and all the corresponding μ-**O** isomers were also considered. Thus, there are six **SO** and μ-**O** pairs in total to be evaluated for the relative stabilities with the series of DFT functionals and basis sets.

B. Basis Sets. As shown in Table 1, basis sets (BS*x*, *x* = 1−6) were constructed using various combinations of basis sets for Fe, S, P, C, O, and H atoms. For Fe, four basis sets were used: (1) Stuttgart relativistic, small core, effective core potential, and associated basis set (Stuttgart RSC 1997 ECP);[28−30] (2)

Table 1. Basis Sets Used in This Investigation

	Fe	S, O (S═O, μ-O)	P, C, O (in CO) C, H (in pdt)	C, H (in PR_3)
BS1	Stuttgart RSC 1997 ECP	cc-pVTZ	cc-pVDZ	cc-pVDZ
BS2	Stuttgart RSC 1997 ECP	cc-pV(T+d)Z+	cc-pVDZ	cc-pVDZ
BS3	Stuttgart RSC 1997 ECP & 2f1g	aug-cc-pVTZ	cc-pVTZ	cc-pVDZ
BS4	LANL2DZ ECP & Couty-Hall 4p	cc-pVTZ	cc-pVDZ	cc-pVDZ
BS5	LANL2DZ ECP & Couty-Hall 4p	cc-pV(T+d)Z+	cc-pVDZ	cc-pVDZ
BS6	cc-pVTZ	cc-pVTZ	cc-pVDZ	cc-pVDZ
BSa	Stuttgart RSC 1997 ECP	D95	D95	D95
BSb	LANL2DZ ECP & Couty-Hall 4p	D95	D95	D95

dx.doi.org/10.1021/ct500594z | J. Chem. Theory Comput. XXXX, XXX, XXX−XXX

Stuttgart RSC 1997 ECP basis set with additional 2f and 1g polarization functions (Stuttgart RSC 1997 ECP & 2f1g);[31] (3) modified Hay-Wadt ECP basis set, in which the two outermost p functions were replaced by reoptimized 4p functions as suggested by Couty and Hall (LANL2DZ ECP & Couty-Hall 4p);[32−35] (4) Dunning's all-electron correlation-consistent polarized valence triple-ζ basis set (cc-pVTZ) for the first row transition metals.[36−38] For S and O (binding to S or Fe), three basis sets were used: (1) cc-pVTZ;[37,38] (2) augmented cc-pVTZ; (3) modified Dunning's correlation-consistent basis sets proposed by Truhlar and co-workers (cc-pV(T+d)Z+), in which the cc-pV(T+d)Z[39] basis set was supplemented with a diffuse sp shell to each non-hydrogenic atom using the standard exponents applied in both the 6-31+G and 6-311+G basis sets.[38,40−42] For C and O (carbonyl groups), P, and C, H in the pdt linker, cc-pVDZ[37,38] was used except for BS2 in that cc-pVTZ was employed. For C and H atoms in the PPh_3 and PMe_3 groups, cc-pVDZ was used in all tested basis sets.

C. Tested DFT Functionals. The DFT functionals used to evaluate the relative stabilities of the **SO** and $\boldsymbol{\mu}$**-O** isomers are listed in Table 2. Pure density functionals with the local (spin) density approximation: LDA,[43] HFB,[44] and SVWN[45,46] and those with the generalized gradient approximation (GGA):[43] BP86 (no exact exchange)[44,47] and B97-D (dispersion correction)[48] were examined. Hybrid GGA functionals B3LYP,[44,49−51] BH&HLYP,[44,49] HSEh1PBE,[52−55] mPW1PW91,[56] MPW1K,[56−58] PBE0,[59,60] and PBEh1PBE[61] were also examined, as were four long-range-corrected hybrid-GGA functionals: CAM-B3LYP,[62] LC-ωPBE,[63−65] ωB97X,[66] and ωB97XD.[67] The double-hybrid functional B2PLYP,[68] which includes exact Hartree−Fock (HF) exchange and a perturbative second-order correlation (PT2), was compared. Finally, the meta-GGA functionals that include the orbital kinetic energy component, Truhlar's pure functional M06-L,[69] and Tao−Perdew−Staroverov−Scuseria (TPSS)[70] functional, as well as the hybrid meta-GGA functionals BMK,[71] M05,[72] M06-HF,[73,74] M06-2X,[75] τ-HCTHhyb,[76] and TPSSh[70] were studied. Because Wheeler et al. reported that the Minnesota suite of functionals were sensitive to the choice of the integration grid,[77] we also examined the M06, M06-L, M06-2X, and M06-HF functionals employing the ultrafine grid, which revealed that the integration grid has little influence on the energies for the present diiron systems.

Table 2. DFT Functionals Used in This Investigation

functional	X^a	type	references
B2PLYP	53	double-hybrid DFT method	68
B3LYP	20	hybrid-GGA	46, 51−53
B97-D	0	GGA-D	50
BH&HLYP	50	hybrid-GGA	46, 51
BMK	42	hybrid meta-GGA	35
BP86	0	GGA	46, 49
CAM-B3LYP	100	long-range-corrected hybrid GGA	62
HFB	0	LSDA	46
HSEh1PBE	25	hybrid-GGA	54−57
LC-ωPBE	100	long-range-corrected hybrid GGA	63−65
M05	28	hybrid meta-GGA	71
M06-HF	100	hybrid meta-GGA	72, 73
M06-L	0	meta-GGA	69
M06-2X	54	hybrid meta-GGA	74
mPW1PW91	25	hybrid-GGA	58
MPW1K	42.8	hybrid-GGA	58−60
PBE0	25	hybrid-GGA	29, 30
PBEh1PBE	25	hybrid-GGA	61
SVWN	0	LSDA	47, 48
τ-HCTHhyb	15	hybrid meta-GGA	75
TPSS	0	meta-GGA	70
TPSSh	10	hybrid meta-GGA	70
ωB97X	100	long-range-corrected hybrid GGA	66
ωB97XD	100	long-range-corrected hybrid GGA-D	67

[a]The X value indicates the percentage of Hartree-Fock exchange.

D. Extrapolating the CCSD Energies. To assess the performance of DFT functionals and basis sets, accurate benchmark data are needed. For this study, the benchmark data were generated by using CCSD calculations. Owing to the large number of atoms for the investigated models, only the smallest models, namely, **1SO** and **1**$\boldsymbol{\mu}$**-O**, were chosen for the CCSD calculations. Further, even for the smallest model, the CCSD level of theory in conjunction with the larger basis sets mentioned in this study would be too computationally demanding. Thus, the larger basis set CCSD relative energies are estimated by using a composite method.[15,16] As has been noted for wave function theory (WFT) methods including electron correlation, the WFT energies can be separated into HF and correlation energy terms (eq 1):[78]

$$E_{\mathrm{CCSD}}^{\mathrm{BS}x} = E_{\mathrm{HF}}^{\mathrm{BS}x} + E_{\mathrm{corr-CCSD}}^{\mathrm{BS}x} \quad (1)$$

Since the HF/BSx energies could be successfully calculated for any x, only the CCSD correlation energies (corr-CCSD) need to be estimated. In general, the corr-CCSD energies that cannot be explicitly calculated can be estimated by using the calculations at lower levels of theory. Thus, the CCSD correlation energies for a larger basis set (BSx) can be estimated from that for a smaller basis set (BS($x-1$)), as shown in eq 2:[78]

$$E_{\mathrm{corr-CCSD}}^{\mathrm{BS}x}(\mathrm{estimated}) = E_{\mathrm{corr-MP2}}^{\mathrm{BS}x} + (E_{\mathrm{corr-CCSD}}^{\mathrm{BS}(x-1)} - E_{\mathrm{corr-MP2}}^{\mathrm{BS}(x-1)}) \quad (2)$$

Herein, MP2 was employed as the lower level of theory; BSx stands for BS1, BS2, and BS4, and BS($x-1$) denotes the smaller basis set used to extrapolate the BSx results (see below and footnote of Table 3 for descriptions of these two smaller basis sets, BSa and BSb). Two cases were considered: (I) in extrapolations for BS1 and BS2 results, the Stuttgart RSC 1997 ECP basis for Fe and the Dunning−Huzinaga full double-ζ (D95) basis sets[79] for S, O, C, and H were used for BS($x-1$) and labeled as BSa; and (II) in extrapolation for BS4 results, the LANL2DZ ECP & Couty-Hall 4p basis set for Fe and D95 for nonmetals were used for BS($x-1$) and labeled as BSb. The estimated CCSD benchmarks for the free energy difference $\Delta G_{\mu\text{O-SO}} = G_{\mathrm{solv}}(\boldsymbol{\mu}\text{-O}) - G_{\mathrm{solv}}(\mathbf{SO})$ between **1SO** and **1**$\boldsymbol{\mu}$**-O** isomers are listed in Table 3. Overall, the extrapolation of the CCSD energies reveals that **1SO** is the thermodynamically favored isomer, especially for BS1 and BS2 results as **1SO** is predicted to be more stable than **1**$\boldsymbol{\mu}$**-O** by 8.94 and 14.76 kcal/mol, respectively. The T1 values for the two isomers are both fairly large (~0.06), values that would suggest that the CCSD results might not be highly accurate. This issue is partly responsible for the extrapolated values having a larger range than one might wish. In spite of the large T1 values, there is no singlet/high-spin instability for either of these isomers, so we have some confidence that the single reference CCSD calculations will produce the correct sign for this energy difference. Thus, we are confident that the main point of the

dx.doi.org/10.1021/ct500594z | J. Chem. Theory Comput. XXXX, XXX, XXX−XXX

Table 3. Estimated CCSD Benchmarks for the Free Energy Difference $\Delta G_{\mu O\text{-}SO}$ [$\Delta G_{\mu O\text{-}SO} = G_{solv}(\mu\text{-O}) - G_{solv}(SO)$] between 1SO and 1$\mu$-O Isomers, Calculated According to eqs 1 and 2

BSx		BSx[a]			BS($x-1$)[a]	
BS1		CCSD/BS1[b]	HF/BS1	corr-MP2/BS1	corr-CCSD/BSa[c]	corr-MP2/BSa
	G_{solv}**1SO**/hartree	−1913.4127	−1909.3316	−4.1764	−2.9943	−3.0895
	G_{solv}**1μ-O**/hartree	−1913.3984	−1909.4315	−3.9780	−2.8972	−2.9083
	$\Delta G_{\mu O\text{-}SO}$/kcal·mol^{-1}	8.94				
BS2		CCSD/BS2	HF/BS2	corr-MP2/BS2	corr-CCSD/BSa[c]	corr-MP2/BSa
	G_{solv}**1SO**/hartree	−1913.4368	−1909.3467	−4.1854	−2.9943	−3.0895
	G_{solv}**1μ-O**/hartree	−1913.4133	−1909.4378	−3.9866	−2.8972	−2.9083
	$\Delta G_{\mu O\text{-}SO}$/kcal·mol^{-1}	14.76				
BS4		CCSD/BS4	HF/BS4	corr-MP2/BS4	corr-CCSD/BSb[c]	corr-MP2/BSb
	G_{solv}**1SO**/hartree	−1911.7418	−1908.3841	−3.3994	−2.4507	−2.4924
	G_{solv}**1μ-O**/hartree	−1911.7408	−1908.4779	−3.2245	−2.3625	−2.3241
	$\Delta G_{\mu O\text{-}SO}$/kcal·mol^{-1}	0.61				

[a]BSx are BS1, BS2 or BS4, while BS($x-1$) are BSa or BSb as shown in Table 1. [b]By following eqs 1 and 2 in the text, the CCSD/BS1 value is calculated as HF/BS1 + corr-MP2/BS1 + corr-CCSD/BSa − corr-MP2/BSa. [c]The calculated T1 values for **1SO** are 0.06550 (BSa) and 0.06369 (BSb), and those for **1μ-O** are 0.05885 (BSa) and 0.05899 (BSb).

Table 4. Structural Features of 1SO and Free Energy Differences $\Delta G_{\mu O\text{-}SO}$ [$\Delta G_{\mu O\text{-}SO} = G_{solv}(\mu\text{-O}) - G_{solv}(SO)$] between 1SO and 1$\mu$-O Isomers, Calculated Using Different Functionals and Basis Sets

	expt	PBE0/BS1[a]	BMK/BS1	PBE0/BS4[a]	PBE0/L-BS1[b]	PBE0/L-BS2[c]	B3LYP/L-BS1[d]	B3LYP/L-BS2[d]	TPSS/L-BS1[d]
				distances/Å					
Fe1−Fe2	2.5765	2.5241	2.5455	2.5083	2.4984	2.4971	2.5483		
Fe1−S1	2.2563	2.2781	2.3502	2.2597	2.2769	2.2853	2.3291		
Fe1−S2(=O)	2.1654	2.1780	2.2572	2.1566	2.1818	2.1839	2.2306		
Fe2−S1	2.2662	2.2665	2.3706	2.2710	2.2871	2.2966			
Fe2−S2(=O)	2.1642	2.1699	2.2704	2.1646	2.1886	2.1918			
S2=O	1.4952	1.4899	1.5008	1.4884	1.5297	1.5134	1.5399		
				angles/deg					
S1−Fe1−S2	82.19	82.55	82.45	82.83	83.46	83.75			
S1−Fe2−S2	82.40	82.11	81.72	82.39	83.07	83.31	82.68		
Fe1−S1−Fe2	69.46	67.48	65.26	67.23	66.38	66.05			
Fe1−S2−Fe2	73.04	70.98	68.42	70.96	69.73	69.59	69.78		
		free energy difference [$\Delta G_{\mu O\text{-}SO} = G_{solv}(\mathbf{1\mu\text{-O}}) - G_{solv}(\mathbf{1SO})$]/kcal·mol^{-1}							
$\Delta G_{\mu O\text{-}SO}$	only **1SO** synthesized	7.13	−33.14	9.17	−2.96	−4.12	−9.60	−10.76	−11.66

[a]BS1 and BS4 are basis sets used in this work, as shown in Table 1. [b]L-BS1 is the basis sets employed in the previous work, which was LANL2DZ ECP & D95 (see ref 12). [c]L-BS2 is the basis sets employed in the previous work, which was LANL2DZ ECP & cc-pVDZ (see ref 12). [d]These results were reported in the previous work (see ref 12).

CCSD calculations is correct, namely, to predict correctly that the **1SO** isomer is more stable than the **1μ-O** isomer.

Initially, we examined the effects of the functionals and basis sets on the geometries of **1SO** and **1μ-O** models to ensure accurate geometries for subsequent calculations. The results for PBE0 and BMK functionals in conjunction with BS1 and BS4 and for the functionals and basis sets employed in the previous work[12] are shown in Table 4. Comparing the calculated results with experimental data reveals that the computational methods have little impact on the geometric parameters. However, the relative stabilities between **1SO** and **1μ-O** isomers fluctuate according to the methods by large amounts (−33.0 to 9.1 kcal/mol); only the PBE0/BS1 result is close to the CCSD evaluation (see Table 3 and Table 5). Therefore, PBE0/BS1 is thought to be reasonable method for the geometric calculations, and the energetic calculations for various functionals will be compared at the PBE0/BS1 geometries. In the present study, all of the equilibrium structures were obtained at the PBE0/BS1 level of theory. At the PBE0/BS1 level of theory, the harmonic vibrational frequencies were calculated to confirm all geometries as minima, and thermodynamic corrections from these gas-phase results were used for the evaluations of the free energies. Single-point electronic energies were recalculated with other functionals and basis sets. Solvent-corrected free energies in toluene were determined on the gas-phase geometries using Truhlar and co-workers' SMD[80] solvation model with toluene as the solvent. All calculations were performed with the Gaussian 09 program package.[81] Unless specified otherwise, the energies mentioned throughout the paper refer to the gas-phase free energies with solvent corrections for toluene.

III. RESULTS AND DISCUSSION

A. Optimized Geometries and Free Energies. Selected geometric parameters of the sulfur−oxygenated (**SO**) and iron−oxygenated (**μ-O**) isomers are collected in Table S1 (Supporting Information) and compared with the experimental data. As shown in Figure 1, the experimental and computational results are in good agreement for the models **1SO**, **2SO$_{ap}$**, and **4SO**. As a whole, the deviation of bond distances is less than 0.1 Å, and the deviation of the bond angles is less than 1.0° except for the Fe1−S2−Fe2 angle in **1SO**, in which the

dx.doi.org/10.1021/ct500594z | J. Chem. Theory Comput. XXXX, XXX, XXX−XXX

Table 5. Relative Energies of the SO and μ-O Isomers

functional[a]		1μ-O-1SO	2μ-O_{ap}-2SO_{ap}	2μ-O_{ba}-2SO_{ba}	3μ-O_{ap}-3SO_{ap}	3μ-O_{ba}-3SO_{ba}	4μ-O-4SO
B2PLYP	ΔE	−23.30	−20.56	−30.17	−21.12	−28.65	−31.40
	ΔH	−23.83	−21.03	−30.68	−21.75	−29.23	−32.10
	ΔG	−22.63	−20.31	−28.22	−21.12	−27.22	−32.03
B3LYP	ΔE	−1.97	2.34	−8.22	1.47	−7.43	−10.35
	ΔH	−2.49	1.86	−8.73	0.84	−8.01	−11.06
	ΔG	−0.96	2.90	−6.31	1.72	−6.14	−11.16
B97-D	ΔE	13.70	19.27	9.28	17.80	8.75	5.49
	ΔH	13.17	18.79	8.77	17.18	8.17	4.79
	ΔG	14.83	19.98	11.03	18.10	9.83	4.41
BH&HLYP	ΔE	−19.40	−16.34	−26.37	−17.00	−24.90	−27.49
	ΔH	−19.92	−16.81	−26.88	−17.62	−25.48	−28.19
	ΔG	−18.68	−16.06	−24.42	−16.96	−23.47	−28.12
BMK	ΔE	−30.88	−28.15	−38.16	−29.74	−36.93	−38.05
	ΔH	−31.40	−28.62	−38.67	−30.36	−37.51	−38.75
	ΔG	−30.13	−27.86	−36.24	−29.73	−35.47	−38.60
BP86	ΔE	8.09	13.05	2.58	12.05	2.85	−0.09
	ΔH	7.56	12.57	2.06	11.42	2.27	−0.79
	ΔG	9.17	13.72	4.28	12.30	3.92	−1.14
CAM-B3LYP	ΔE	−5.01	−0.69	−11.47	−1.66	−10.65	−13.36
	ΔH	−5.53	−1.17	−11.99	−2.29	−11.23	−14.07
	ΔG	−4.09	−0.21	−9.53	−1.47	−9.28	−14.08
HFB	ΔE	−5.05	−1.08	−10.17	−1.76	−9.53	−13.16
	ΔH	−5.58	−1.55	−10.69	−2.39	−10.11	−13.86
	ΔG	−3.94	−0.38	−8.35	−1.48	−8.41	−14.17
HSEh1PBE	ΔE	5.33	9.88	−0.69	9.05	−0.23	−3.12
	ΔH	4.81	9.40	−1.21	8.42	−0.81	−3.83
	ΔG	6.27	10.37	1.11	9.22	0.99	−3.96
LC-ωPBE	ΔE	4.95	9.86	−1.22	8.93	−0.70	−4.03
	ΔH	4.42	9.39	−1.74	8.30	−1.28	−4.73
	ΔG	5.82	10.30	1.18	9.07	0.60	−4.76
M05	ΔE	17.44	23.74	11.73	22.52	12.16	9.33
	ΔH	16.92	23.26	11.22	21.89	11.58	8.63
	ΔG	18.52	24.39	13.54	22.80	13.32	8.35
M06-HF	ΔE	−49.48	−46.86	−56.04	−47.00	−54.36	−56.46
	ΔH	−50.00	−47.33	−56.55	−47.62	−54.94	−57.17
	ΔG	−49.11	−46.94	−54.17	−47.22	−52.81	−56.94
M06-L	ΔE	4.76	9.71	−0.47	8.50	−1.09	−4.67
	ΔH	4.24	9.23	−0.99	7.87	−1.67	−5.38
	ΔG	5.86	10.41	1.26	8.80	−0.01	−5.72
M06-2X	ΔE	−16.10	−13.45	−21.67	−14.13	−21.53	−23.95
	ΔH	−16.63	−13.92	−22.19	−14.75	−22.11	−24.65
	ΔG	−15.47	−13.20	−19.89	−12.43	−20.27	−24.71
mPW1PW91	ΔE	4.77	9.18	−1.24	8.45	−0.80	−3.89
	ΔH	4.25	8.71	−1.76	7.83	−1.38	−4.59
	ΔG	5.70	9.68	0.57	8.64	0.45	−4.71
MPW1K	ΔE	−3.63	0.01	−10.13	−0.55	−9.30	−12.28
	ΔH	−4.15	−0.46	−10.65	−1.17	−9.88	−12.98
	ΔG	−2.86	0.34	−8.29	−0.49	−7.96	−12.98
PBE0	ΔE	6.20	10.78	0.35	9.94	0.69	−2.21
	ΔH	5.67	10.31	−0.17	9.32	0.11	−2.92
	ΔG	7.13	11.27	2.15	10.11	1.92	−3.05
PBEh1PBE	ΔE	5.32	9.87	−0.68	9.03	−0.24	−3.13
	ΔH	4.79	9.39	−1.20	8.40	−0.82	−3.84
	ΔG	6.25	10.36	1.12	9.20	0.99	−3.97
SVWN	ΔE	16.33	22.34	10.49	20.86	10.54	8.49
	ΔH	15.80	21.87	9.97	20.24	9.96	7.79
	ΔG	17.45	23.05	12.21	21.15	11.64	7.45
τ-HCTHhyb	ΔE	1.49	5.77	−4.56	5.00	−3.90	−6.88
	ΔH	0.96	5.29	−5.08	4.37	−4.48	−7.59
	ΔG	2.46	6.30	−2.76	5.19	−2.70	−7.75
TPSS	ΔE	3.08	8.24	−2.32	7.33	−2.22	−5.25

dx.doi.org/10.1021/ct500594z | J. Chem. Theory Comput. XXXX, XXX, XXX−XXX

Table 5. continued

functional[a]		1μ-O-1SO	2μ-O$_{ap}$-2SO$_{ap}$	2μ-O$_{ba}$-2SO$_{ba}$	3μ-O$_{ap}$-3SO$_{ap}$	3μ-O$_{ba}$-3SO$_{ba}$	4μ-O-4SO
	ΔH	2.56	7.77	−2.84	6.70	−2.80	−5.96
	ΔG	4.14	8.90	−0.62	7.57	−1.16	−6.27
TPSSh	ΔE	2.40	7.34	−3.23	6.54	−3.05	−6.19
	ΔH	1.88	6.86	−3.75	5.92	−3.63	−6.89
	ΔG	3.41	7.93	−1.48	6.76	−1.91	−7.11
ωB97X	ΔE	−2.37	1.69	−8.29	0.63	−7.69	−10.22
	ΔH	−2.89	1.22	−8.80	0.01	−8.27	−10.93
	ΔG	−1.56	2.07	−6.46	0.71	−6.42	−10.99
ωB97XD	ΔE	1.47	5.29	−3.85	4.43	−3.61	−6.61
	ΔH	0.95	4.81	−4.36	3.81	−4.19	−7.31
	ΔG	2.36	5.73	−2.00	4.58	−2.32	−7.37

[a]Calculated at the various functionals/BS1 levels of theory. Energies are reported in kcal/mol.

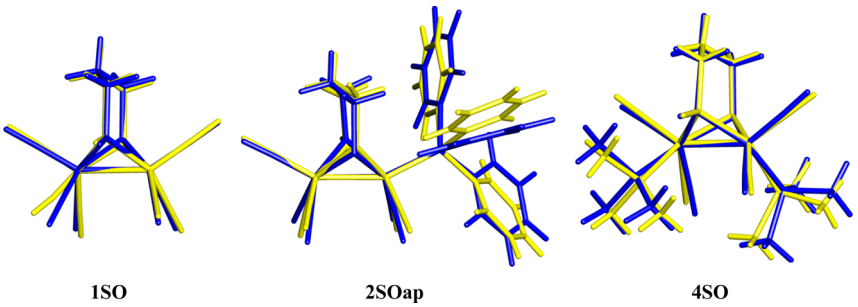

Figure 1. Superpositions of optimized geometries (blue) with the crystal structures (yellow) of the sulfur−oxygenated complexes (**1SO**, **2SO$_{ap}$**, and **4SO**).

calculated value is 2.1° smaller than that in the crystal structure. For the **SO** species, the calculated average Fe−Fe bond length (2.547 Å) is slightly longer than that of the unoxygenated precursors (2.531 Å).[82−84] In contrast, the insertion of O atom in the ***μ*-O** species breaks the Fe−Fe bond, which lengthens by ∼0.3 Å on average. In addition, the relative position of the phosphine group in the monosubstituted species has an influence on the geometries. Changing PR_3 groups from an apical to a basal site slightly decreases the Fe−Fe distance in the ***μ*-O** complexes, whereas this change increases the Fe−Fe bond by ∼0.6 and 0.4 Å for **2SO** and **3SO**, respectively.

The free energy differences between **1SO** and **1*μ*-O** isomers, as calculated at the various functionals and basis sets, are presented in Figure 2 and Supporting Information, Table S2. One can see that these energy differences vary with different functionals by over 70 kcal/mol, whereas the variation with basis sets is over a smaller range, averaging about 12 kcal/mol (except for the result obtained at the BMK/BS6 level of theory).

B. Influence of the Basis Sets on the Relative Stabilities of SO and *μ*-O Isomers. Liu et al. reported that **1*μ*-O** was lower in energy than **1SO** with $\Delta G_{\mu\text{O-SO}}$ of −9.60, −10.76, and −11.66 kcal/mol using B3LYP/D95&LANL2DZ (L-BS1), B3LYP/cc-pVDZ&LANL2DZ (L-BS2), and TPSS/cc-pVDZ&LANL2DZ (L-BS2), respectively.[12] However, replacing the double-ζ cc-pVDZ basis set on S and O (L-BS2) by the triple-ζ cc-pVTZ one (BS4) results in $\Delta G_{\mu\text{O-SO}}$ of 0.71 kcal/mol for B3LYP and 5.27 kcal/mol for TPSS (see Figure 2 and Table S2, Supporting Information). Similar results for these basis sets are also reported in Table 4 for the PBE0 level of theory.

In general, the basis sets tested herein present parallel trends for all of the different functionals. The additional polarization functions and diffuse functions in BS2 stabilize the **1SO** isomer and make the energy differences $\Delta G_{\mu\text{O-SO}}$ more positive. Supporting Information, Table S2, shows that $\Delta G_{\mu\text{O-SO}}$

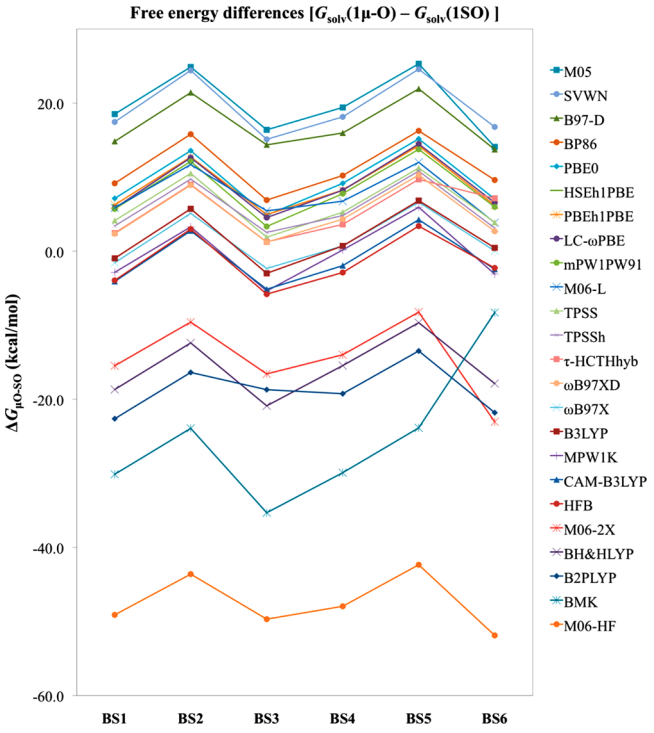

Figure 2. Effect of basis sets on the free energy difference $\Delta G_{\mu\text{O-SO}}$ [$\Delta G_{\mu\text{O-SO}} = G_{solv}(\mu\text{-O}) - G_{solv}(\text{SO})$] between **1SO** and **1*μ*-O** isomers, as calculated with various functionals and basis sets. Energies are reported in kcal/mol.

dx.doi.org/10.1021/ct500594z | J. Chem. Theory Comput. XXXX, XXX, XXX−XXX

increases by 6.4 kcal/mol on average. The results for the largest basis set, BS3, are quite similar to those for BS1, so the augmentation of basis functions on light atoms and the extra polarization functions on the metals are not particular important. Further evidence that details of the metal basis set are not particularly important are shown by the comparisons of BS1, BS4, and BS6, where similar energy differences are seen (Figure 2 and Supporting Information, Table S2).

Notably, there is a large increase in $\Delta G_{\mu O\text{-}SO}$ when replacing the cc-pVDZ by cc-pVTZ, and a further increase when this basis set is replaced by cc-pV(T+d)Z+. To explore what appears to be the most important basis set issue with respect to which atom, S or O, has more influence on this difference, we used the PBE0 functional to examine a series of basis sets in which the LANL2DZ ECP & Couty−Hall 4p was set for Fe and different basis sets were set for S and O (binding to S or Fe). The calculated results are presented in Table S3 (Supporting Information). It can be noted that adding more than one d polarization function and one f polarization function on sulfur atoms, cc-pVDZ to cc-pVTZ, results in large increases in $\Delta G_{\mu O\text{-}SO}$, (13 to 15 kcal/mol); of these changes, the additional d function seems most important. Extra polarization functions on the oxygen atom have a smaller impact on $\Delta G_{\mu O\text{-}SO}$ (~1 kcal/mol). Moreover, additional diffuse functions on S led to a small increase in $\Delta G_{\mu O\text{-}SO}$ (1 to 2 kcal/mol), whereas a relatively large decrease (~5 kcal/mol) is found when the diffuse functions are added on O. These details give a reasonable explanation for the observed trends in $\Delta G_{1\mu O\text{-}1SO}$.

The effect of basis sets on the relative stabilities for the larger substituted isomeric species (i.e., models **2**, **3**, and **4**) are plotted in Supporting Information, Figure S1, where trends similar to those observed for the models **1** are apparent. As a whole, extra polarization functions on the basis sets for sulfur atoms appear to be essential for the correct treatment of the S═O bond. Relative to the importance of these additional functions for S, basis sets for the metals and other light atoms have a significantly smaller influence on $\Delta G_{\mu O\text{-}SO}$. Thus, extra polarization functions on S atoms are essential to determine the oxygenation site for these and related diron complexes.

C. Influence of the DFT Functionals on the Relative Stabilities of SO and *μ*-O Isomers. All subsequent discussions are based on the results calculated at the functional/BS1 level of theory. The relative electronic energies, enthalpies, and solvent-corrected free energies of the **SO** and ***μ*-O** isomers are presented in Table 5, and the free energy differences are plotted in Figures 3 and 4. Our studies reveal that the relative stabilities between ***μ*-O** and **SO** isomers are much more sensitive to the choice of the functionals than the initial differences between B3LYP and TPSS would have suggested[12] As shown in Figure 3, the wide range of functionals tested here produce a huge variation in the free energy differences $\Delta G_{\mu O\text{-}SO} = [G_{solv}(\mathbf{1}\mu\text{-}\mathbf{O}) - G_{solv}(\mathbf{1SO})]$, from −49.1 to 18.5 kcal/mol. In spite of the seemingly wild fluctuations of these energy differences, some trends are visible. The closely related HSEh1PBE, PBEh1PBE, and PBE0 functionals with 25% HF exchange give similar positive $\Delta G_{\mu O\text{-}SO}$ values, predicting that **1SO** is the thermodynamically favored isomer. Functionals with larger amounts of HF exchange such as B2PLYP, BH&HLYP, BMK, M06-HF, and M06-2X give $\Delta G_{\mu O\text{-}SO}$ values that are quite negative. To be fair, we note that M06-HF, which produces the most negative value at −49.1, is not recommended for transition metal systems; however, even if one removes this outlier the range is still

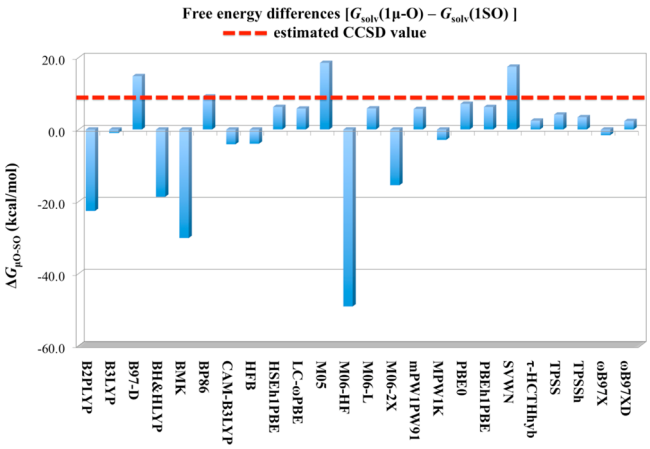

Figure 3. Effect of DFT functionals on the free energy difference $\Delta G_{\mu O\text{-}SO}$ $[\Delta G_{\mu O\text{-}SO} = G_{solv}(\boldsymbol{\mu}\text{-}\mathbf{O}) - G_{solv}(\mathbf{SO})]$ between **1SO** and **1*μ*-O** isomers, as calculated using BS1 basis set and compared with the estimated CCSD value. Energies are reported in kcal/mol. Note that the extreme negative outlier, M06-HF, would not have been expected to perform well as it is not recommended for transition metal systems.

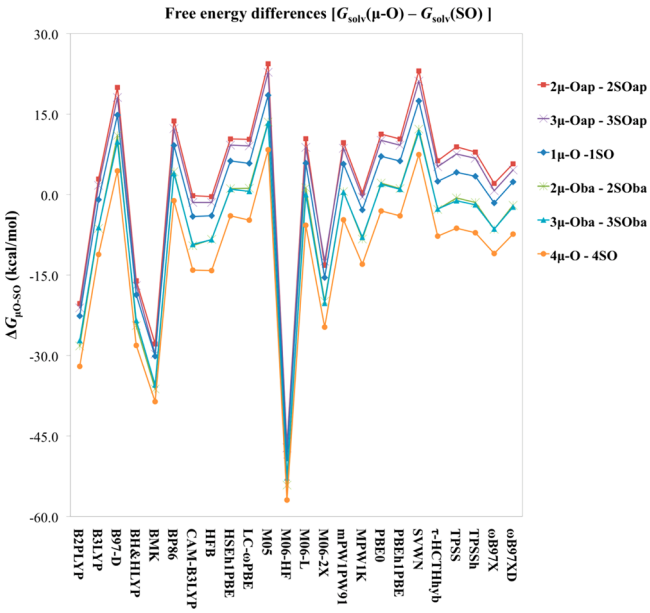

Figure 4. Effect of DFT functionals on the free energy difference $\Delta G_{\mu O\text{-}SO}$ $[\Delta G_{\mu O\text{-}SO} = G_{solv}(\boldsymbol{\mu}\text{-}\mathbf{O}) - G_{solv}(\mathbf{SO})]$ between **SO** and ***μ*-O** isomers, as calculated using BS1 basis set. Energies are reported in kcal/mol.

nearly 50 kcal/mol. Comparing the related B3LYP and BH&HLYP shows that increasing the HF exchange from 20% to 50% decreases the free energy differences from −0.96 to −18.68 kcal/mol. These results parallel other comparisons[85] in that they show similar strong dependence in the degree of pure exchange. Further, comparing the results calculated for BP86 vs B97-D and ωB97X vs ωB97X-D reveals that dispersion corrections increase the value of $\Delta G_{\mu O\text{-}SO}$ by 5 kcal/mol. Figure 3 also presents the estimated CCSD value for this basis set, which predicts that **1SO** is thermodynamically favored by 8.94 kcal/mol. According to this benchmark, BP86 performs the best among all 24 tested functionals with an "error" of 0.2 kcal/mol, while PBE0 is the second best with an error of 1.8 kcal/mol. The results calculated with the HSEh1PBE,

dx.doi.org/10.1021/ct500594z | J. Chem. Theory Comput. XXXX, XXX, XXX−XXX

PBEh1PBE, M06-L, LC-ωPBE, and mPW1PW91 functionals are also in fairly good agreement with this CCSD benchmark, while the TPSS, TPSSh, and B97-D functionals give a fair performance with absolute deviations from CCSD of less than 6 kcal/mol (Table 5).

Figure 4 shows the influences of tested functionals on the relative stabilities for the larger substituted isomeric species (i.e., models **2**, **3**, and **4**), where trends similar to those of model **1** are observed. Interestingly, the relative position of the PR_3 (R = Ph and Me) substituent group has an impact on the free energy differences $\Delta G_{\mu\text{O-SO}}$. Figure 4 shows that the apical arrangement of PPh_3 (R = Ph and Me) group stabilizes the **SO** isomers and makes $\Delta G_{\mu\text{O-SO}}$ more positive, as compared with the results of the unsubstituted models (i.e., **1SO** and **1μ-O**). In contrast, the rotation of the $Fe(PR_3)(CO)_2$ (R = Ph and Me) group that moves PR_3 from the apical to basal position stabilizes the **μ-O** isomers. For the **4SO** and **4μ-O** isomers, in which two PMe_3 groups are located in the transoid basal sites, $\Delta G_{\mu\text{O-SO}}$ is decreased by 10.0 kcal/mol, and only the calculations with the B97-D, M05, and SVWN functionals show that **4SO** is more stable than **4μ-O**. Figure 4 and Table 5 show that the variations of $\Delta G_{\mu\text{O-SO}}$ with the relative positions of PR_3 (R = Ph and Me) group are less than 16 kcal/mol, far less than the influence caused by the variations of the functionals, but still significant chemically.

To sum up, the DFT functionals have a great influence on the predicted relative stabilities for these diiron complexes. The M05, B97-D, and SVWN functionals predict that **SO** isomers are more stable than **μ-O** species but may overestimate the relative free energies. BP86, PBE0, HSEh1PBE, PBEh1PBE, mPW1PW91, and M06-L functionals appear to have the best performance such that the **SO** isomers are thermodynamically favored but not too strongly. In contrast, the B2PLYP, BH&HLYP, BMK, M06-HF, and M06-2X functionals with high percentage of HF exchange show quite negative $\Delta G_{\mu\text{O-SO}}$ values, especially for M06-2X.

D. Influence of the Computational Methods on the Relative Stabilities of Apical and Basal PR_3 Isomers. Unlike the sensitivity to computational methods for the relative stabilities of **SO** and **μ-O** isomeric species, the energy differences between apical and basal PMe_3 and PPh_3 isomers present a relatively small response to the theoretical methods. Detailed results are available in Supporting Information, Tables S4 and S5. Generally, the functionals again have a greater influence on the energy differences [$\Delta G_{\text{ba-ap}} = G_{\text{solv}}(\mathbf{SO}_{\text{ba}}) - G_{\text{solv}}(\mathbf{SO}_{\text{ap}})$ or $G_{\text{solv}}(\mu\text{-}\mathbf{O}_{\text{ba}}) - G_{\text{solv}}(\mu\text{-}\mathbf{O}_{\text{ap}})$] than the basis sets. For the **2SO** species, most functionals show that $\mathbf{2SO}_{\text{ap}}$ is more stable than $\mathbf{2SO}_{\text{ba}}$, in agreement with the experiment, except BP86, HFB, SVWN, and TPSS, for which $\mathbf{2SO}_{\text{ba}}$ is slightly lower in energy (Supporting Information, Table S4). Unlike the **2SO** species, for **3SO** only the B2PLYP, BH&HLYP, BMK, M06-HF, and M06-2X functionals (except BS5) calculate the $\mathbf{3SO}_{\text{ap}}$ to be slightly lower in energy than $\mathbf{3SO}_{\text{ba}}$ (Supporting Information, Table S5). For the **2μ-O** species, all of the tested theoretical methods except for M06-HF/BSx predict that $\mathbf{2}\mu\text{-}\mathbf{O}_{\text{ba}}$ is the thermodynamically favored isomer with $\Delta G_{\text{ba-ap}}$ ranging from −2.7 to −11.6 kcal/mol, while for **3μ-O**, all of the tested methods reveal that $\mathbf{3}\mu\text{-}\mathbf{O}_{\text{ba}}$ is more stable than $\mathbf{3}\mu\text{-}\mathbf{O}_{\text{ap}}$.

IV. CONCLUSIONS

In the present study, 24 DFT functionals and six basis sets were examined to evaluate the influence of the computational methods on the relative stabilities of a series of iron-oxygenated (**μ-O**) and sulfur-oxygenated (**SO**) isomers of diiron complexes, which are important models for hydrogenases and their reactions with oxygen.

As for the effect of basis sets, the basis sets for S and O (binding to S or Fe) appear to be more important to the free-energy differences than the basis sets for iron, and it appears that adding more than one d polarization function is necessary on the "active" sulfur atoms.

In contrast to the influence of basis sets, the functionals play a determinative role, and the free energy differences [$\Delta G_{\mu\text{O-so}} = G_{\text{solv}}(\mu\text{-}\mathbf{O}) - G_{\text{solv}}(\mathbf{SO})$] span a huge range of over 70 kcal/mol. Taking **1SO** and **1μ-O** isomers as examples, the CCSD calculations and 14 functionals predict that the **1SO** is the thermodynamically favored isomer, while 10 functionals predict the opposite. In comparison with the CCSD benchmarks, BP86 and PBE0 show the best performance, whereas functionals with high percentages of HF exchange such as B2PLYP, BMK, and M06-2X perform very poorly. Trends similar to those observed for model **1** are also observed for the larger substituted isomeric species. Moreover, the relative position of the PR_3 (R = Ph and Me) substituent group has a small impact on the free energy differences. In a brief examination of the relative energies of binding a single triplet-state O atom to S to form the **1SO** isomer or to Fe_2 to form the **1μ-O** isomer, over 70% of the variation described above is due to the binding to the Fe_2. Thus, a large fraction of the error may lie with the various functionals' ability to correctly predict the strength of the Fe−Fe bond in **1**.

From the assessments, we recommend the BP86 or PBE0 functionals for modeling the oxygenated isomers of these diiron complexes. One might also expect that these functionals would be good choices for reactions involving transfer of a first-row atom or fragment from a transition metal to a second- or third-row main-group molecule, such as O transfer from a Mo═O complex to PR_3.

■ ASSOCIATED CONTENT

Supporting Information

Table of some selected geometric parameters of the sulfur−oxygenated (**SO**) and iron−oxygenated (**μ-O**) isomers calculated on the basis of PBE0/BS1. Tables of the relative free energies between apical and basal isomers for **2SO**, **2μ-O**, **3SO**, and **3μ-O**, calculated using different functionals and basis sets. Figure of the effect of basis sets on the free energy difference between **SO** and **μ-O** isomers as calculated with various functionals and basis sets. Cartesian coordinates of optimized structures. This material is available free of charge via the Internet at http://pubs.acs.org.

■ AUTHOR INFORMATION

Corresponding Author

*E-mail: mbhall@tamu.edu.

Notes

The authors declare no competing financial interest.

■ ACKNOWLEDGMENTS

We acknowledge the financial support of the National Science Foundation (CHE-0910552 and CHE-1300787) and The Welch Foundation (A-0648). We acknowledge a grant of computer time from Texas A&M University's Supercomputer Facility. We thank one of the referees for confirming that there is no singlet/high-spin instability.

REFERENCES

(1) Adams, M. W. *Biochim. Biophys. Acta* **1990**, *1020*, 115−145.
(2) Fontecilla-Camps, J. C.; Volbeda, A.; Cavazza, C.; Nicolet, Y. *Chem. Rev.* **2007**, *107*, 4273−4303.
(3) Siegbahn, P. E.; Tye, J. W.; Hall, M. B. *Chem. Rev.* **2007**, *107*, 4414−4435.
(4) Tard, C.; Pickett, C. J. *Chem. Rev.* **2009**, *109*, 2245−2274.
(5) Surawatanawong, P.; Tye, J. W.; Darensbourg, M. Y.; Hall, M. B. *Dalton Trans.* **2010**, *39*, 3093−3104.
(6) Vincent, K. A.; Parkin, A.; Lenz, O.; Albracht, S. P.; Fontecilla-Camps, J. C.; Cammack, R.; Friedrich, B.; Armstrong, F. A. *J. Am. Chem. Soc.* **2005**, *127*, 18179−18189.
(7) Ludwig, M.; Cracknell, J. A.; Vincent, K. A.; Armstrong, F. A.; Lenz, O. *J. Biol. Chem.* **2009**, *284*, 465−477.
(8) Armstrong, F. A.; Belsey, N. A.; Cracknell, J. A.; Goldet, G.; Parkin, A.; Reisner, E.; Vincent, K. A.; Wait, A. F. *Chem. Soc. Rev.* **2009**, *38*, 36.
(9) Goldet, G.; Brandmayr, C.; Stripp, S. T.; Happe, T.; Cavazza, C.; Fontecilla-Camps, J. C.; Armstrong, F. A. *J. Am. Chem. Soc.* **2009**, *131*, 14979−14989.
(10) Farmer, P. J.; Verpeaux, J.-N.; Amatore, C.; Darensbourg, M. Y.; Musie, G. *J. Am. Chem. Soc.* **1994**, *116*, 9355−9356.
(11) Grapperhaus, C. A.; Darensbourg, M. Y. *Acc. Chem. Res.* **1998**, *31*, 451−459.
(12) Liu, T.; Li, B.; Singleton, M. L.; Hall, M. B.; Darensbourg, M. Y. *J. Am. Chem. Soc.* **2009**, *131*, 8296−8307.
(13) Kurtz, D. M. *Chem. Rev.* **1990**, *90*, 585−606.
(14) Tshuva, E. Y.; Lippard, S. J. *Chem. Rev.* **2004**, *104*, 987−1012.
(15) Beddie, C.; Hall, M. B. *J. Phys. Chem. A* **2006**, *110*, 1416−1425.
(16) Zhao, Y.; Truhlar, D. G. *J. Chem. Theory Comput.* **2009**, *5*, 324−333.
(17) Vastine, B. A.; Webster, C. E.; Hall, M. B. *J. Chem. Theory Comput.* **2007**, *3*, 2268−2281.
(18) Quintal, M. M.; Karton, A.; Iron, M. A.; Boese, A. D.; Martin, J. M. L. *J. Phys. Chem. A* **2005**, *110*, 709−716.
(19) George, M. W.; Hall, M. B.; Portius, P.; Renz, A. L.; Sun, X. Z.; Towrie, M.; Yang, X. *Dalton Trans.* **2011**, *40*, 1751−1757.
(20) Bryantsev, V. S.; Diallo, M. S.; van Duin, A. C. T.; Goddard, W. A. *J. Chem. Theory Comput.* **2009**, *5*, 1016−1026.
(21) Marom, N.; Tkatchenko, A.; Scheffler, M.; Kronik, L. *J. Chem. Theory Comput.* **2009**, *6*, 81−90.
(22) Bühl, M.; Kabrede, H. *J. Chem. Theory Comput.* **2006**, *2*, 1282−1290.
(23) Yang, K.; Zheng, J.; Zhao, Y.; Truhlar, D. G. *J. Chem. Phys.* **2010**, *132*, 164117.
(24) Schultz, N. E.; Zhao, Y.; Truhlar, D. G. *J. Phys. Chem. A* **2005**, *109*, 4388−4403.
(25) Zhao, Y.; Truhlar, D. G. *J. Chem. Theory Comput.* **2006**, *2*, 1009−1018.
(26) Shamov, G. A.; Schreckenbach, G.; Budzelaar, P. H. M. *J. Chem. Theory Comput.* **2010**, *6*, 3442−3455.
(27) Jabłoński, M.; Palusiak, M. *J. Phys. Chem. A* **2010**, *114*, 2240−2244.
(28) Andrae, D.; Haussermann, U.; Dolg, M.; Stoll, H.; Preuss, H. *Theor. Chim. Acta* **1990**, *77*, 123−141.
(29) Basis sets were obtained from the Extensible Computational Chemistry Environment Basis Set Database, v., as developed and distributed by the Molecular Science Computing Facility, Environmental and Molecular Sciences Laboratory, which is part of the Pacific Northwest Laboratory, P.O. Box 999, Richland, WA 99352, and funded by the U.S. Department of Energy. The Pacific Northwest Laboratory is a multiprogram laboratory operated by Battelle Memorial Institute for the U.S. Department of Energy under Contract No. DE-AC06−76.RLO 1830. Contact Karen Schuchardt for further information. http://www.emsl.pnl.gov/forms/basisform.html.
(30) Bergner, A.; Dolg, M.; Kuchle, W.; Stoll, H.; Preuss, H. *Mol. Phys.* **1993**, *80*, 1431−1441.
(31) Martin, J. M. L.; Sundermann, A. *J. Chem. Phys.* **2001**, *114*, 3408−3420.
(32) Hay, P. J.; Wadt, W. R. *J. Chem. Phys.* **1985**, *82*, 270−283.
(33) Hay, P. J.; Wadt, W. R. *J. Chem. Phys.* **1985**, *82*, 299−310.
(34) Wadt, W. R.; Hay, P. J. *J. Chem. Phys.* **1985**, *82*, 284−298.
(35) Couty, M.; Hall, M. B. *J. Comput. Chem.* **1996**, *17*, 1359−1370.
(36) Balabanov, N. B.; Peterson, K. A. *J. Chem. Phys.* **2005**, *123*, 064107.
(37) Dunning, T. H. *J. Chem. Phys.* **1989**, *90*, 1007−1023.
(38) Woon, D. E.; Dunning, T. H. *J. Chem. Phys.* **1993**, *98*, 1358−1371.
(39) Dunning, T. H.; Peterson, K. A.; Wilson, A. K. *J. Chem. Phys.* **2001**, *114*, 9244−9253.
(40) Clark, T.; Chandrasekhar, J.; Spitznagel, G. W.; Schleyer, P. V. *J. Comput. Chem.* **1983**, *4*, 294−301.
(41) Papajak, E.; Leverentz, H. R.; Zheng, J. J.; Truhlar, D. G. *J. Chem. Theory Comput.* **2009**, *5*, 3330−3330.
(42) Papajak, E.; Leverentz, H. R.; Zheng, J. J.; Truhlar, D. G. *J. Chem. Theory Comput.* **2009**, *5*, 1197−1202.
(43) Sousa, S. F.; Fernandes, P. A.; Ramos, M. J. *J. Phys. Chem. A* **2007**, *111*, 10439−10452.
(44) Becke, A. D. *Phys. Rev. A* **1988**, *38*, 3098−3100.
(45) Slater, J. C. *The Self-Consistent Field for Molecular and Solids, Quantum Theory of Molecular and Solids*; McGraw-Hill: New York, 1974; Vol. *4*.
(46) Vosko, S. H.; Wilk, L.; Nusair, M. *Can. J. Phys.* **1980**, *58*, 1200−1211.
(47) Perdew, J. P. *Phys. Rev. B* **1986**, *33*, 8822−8824.
(48) Grimme, S. *J. Comput. Chem.* **2006**, *27*, 1787−1799.
(49) Lee, C. T.; Yang, W. T.; Parr, R. G. *Phys. Rev. B* **1988**, *37*, 785−789.
(50) Becke, A. D. *J. Chem. Phys.* **1993**, *98*, 5648−5652.
(51) Stephens, P. J.; Devlin, F. J.; Chabalowski, C. F.; Frisch, M. J. *J. Phys. Chem.* **1994**, *98*, 11623−11627.
(52) Heyd, J.; Scuseria, G. E. *J. Chem. Phys.* **2004**, *120*, 7274−7280.
(53) Heyd, J.; Peralta, J. E.; Scuseria, G. E.; Martin, R. L. *J. Chem. Phys.* **2005**, *123*, 174101.
(54) Heyd, J.; Scuseria, G. E. *J. Chem. Phys.* **2004**, *121*, 1187−1192.
(55) Heyd, J.; Scuseria, G. E.; Ernzerhof, M. *J. Chem. Phys.* **2006**, *124*, 219906.
(56) Adamo, C.; Barone, V. *J. Chem. Phys.* **1998**, *108*, 664−675.
(57) Becke, A. D. *J. Chem. Phys.* **1996**, *104*, 1040−1046.
(58) Zhao, Y.; Truhlar, D. G. *J. Phys. Chem. A* **2004**, *108*, 6908−6918.
(59) Perdew, J. P.; Burke, K.; Ernzerhof, M. *Phys. Rev. Lett.* **1996**, *77*, 3865−3868.
(60) Adamo, C.; Barone, V. *J. Chem. Phys.* **1999**, *110*, 6158−6170.
(61) Ernzerhof, M.; Perdew, J. P. *J. Chem. Phys.* **1998**, *109*, 3313−3320.
(62) Yanai, T.; Tew, D. P.; Handy, N. C. *Chem. Phys. Lett.* **2004**, *393*, 51−57.
(63) Vydrov, O. A.; Scuseria, G. E. *J. Chem. Phys.* **2006**, *125*, 234109.
(64) Vydrov, O. A.; Heyd, J.; Krukau, A. V.; Scuseria, G. E. *J. Chem. Phys.* **2006**, *125*, 074106.
(65) Vydrov, O. A.; Scuseria, G. E.; Perdew, J. P. *J. Chem. Phys.* **2007**, *126*, 154109.
(66) Chai, J. D.; Head-Gordon, M. *J. Chem. Phys.* **2008**, *128*, 084106.
(67) Chai, J. D.; Head-Gordon, M. *Phys. Chem. Chem. Phys.* **2008**, *10*, 6615−6620.
(68) Grimme, S. *J. Chem. Phys.* **2006**, *124*, 034108.
(69) Zhao, Y.; Truhlar, D. G. *J. Chem. Phys.* **2006**, *125*, 194101.
(70) Tao, J. M.; Perdew, J. P.; Staroverov, V. N.; Scuseria, G. E. *Phys. Rev. Lett.* **2003**, *91*, 146401.
(71) Boese, A. D.; Martin, J. M. L. *J. Chem. Phys.* **2004**, *121*, 3405−3416.
(72) Zhao, Y.; Schultz, N. E.; Truhlar, D. G. *J. Chem. Phys.* **2005**, *123*, 194101.
(73) Zhao, Y.; Truhlar, D. G. *J. Phys. Chem. A* **2006**, *110*, 5121−5129.
(74) Zhao, Y.; Truhlar, D. G. *J. Phys. Chem. A* **2006**, *110*, 13126−13130.
(75) Zhao, Y.; Truhlar, D. G. *Theor. Chem. Acc.* **2008**, *120*, 215−241.

(76) Boese, A. D.; Handy, N. C. *J. Chem. Phys.* **2002**, *116*, 9559−9569.
(77) Wheeler, S. E.; Houk, K. N. *J. Chem. Theory Comput.* **2010**, *6*, 395−404.
(78) Zhao, Y.; Truhlar, D. G. *J. Phys. Chem. A* **2005**, *109*, 4209−4212.
(79) Dunning, T. H. H., P, J. In *Modern Theoretical Chemistry;* Schaefer, H. F., III, Ed.; Plenum: New York, 1976; Vol. 3; pp 1−28.
(80) Marenich, A. V.; Cramer, C. J.; Truhlar, D. G. *J. Phys. Chem. B* **2009**, *113*, 6378−6396.
(81) Frisch, M. J. T., G, W.; Schlegel, H. B.; Scuseria, G. E.; Robb, M. A.; Cheeseman, J. R.; Scalmani, G.; Barone, V.; Mennucci, B.; Petersson, G. A.; Nakatsuji, H.; Caricato, M.; Li, X.; Hratchian, H. P.; Izmaylov, A. F.; Bloino, J.; Zheng, G.; Sonnenberg, J. L.; Hada, M.; Ehara, M.; Toyota, K.; Fukuda, R.; Hasegawa, J.; Ishida, M.; Nakajima, T.; Honda, Y.; Kitao, O.; Nakai, H.; Vreven, T.; Montgomery, J. A., Jr.; Peralta, J. E.; Ogliaro, F.; Bearpark, M.; Heyd, J. J.; Brothers, E.; Kudin, K. N.; Staroverov, V. N.; Kobayashi, R.; Normand, J.; Raghavachari, K.; Rendell, A.; Burant, J. C.; Iyengar, S. S.; Tomasi, J.; Cossi, M.; Rega, N.; Millam, N. J.; Klene, M.; Knox, J. E.; Cross, J. B.; Bakken, V.; Adamo, C.; Jaramillo, J.; Gomperts, R.; Stratmann, R. E.; Yazyev, O.; Austin, A. J.; Cammi, R.; Pomelli, C.; Ochterski, J. W.; Martin, R. L.; Morokuma, K.; Zakrzewski, V. G.; Voth, G. A.; Salvador, P.; Dannenberg, J. J.; Dapprich, S.; Daniels, A. D.; Farkas, Ö.; Foresman, J. B.; Ortiz, J. V.; Cioslowski, J.; Fox, D. J. *Gaussian 09,* Revision A.02; Gaussian, Inc.: Wallingford, CT, 2009.
(82) Lyon, E. J.; Georgakaki, I. P.; Reibenspies, J. H.; Darensbourg, M. Y. *Angew. Chem., Int. Ed.* **1999**, *38*, 3178−3180.
(83) Zhao, X.; Georgakaki, I. P.; Miller, M. L.; Yarbrough, J. C.; Darensbourg, M. Y. *J. Am. Chem. Soc.* **2001**, *123*, 9710−9711.
(84) Li, P.; Wang, M.; He, C. J.; Li, G. H.; Liu, X. Y.; Chen, C. N.; Akermark, B.; Sun, L. C. *Eur. J. Inorg. Chem.* **2005**, 2506−2513.
(85) (a) Radoń, M. *Phys. Chem. Chem. Phys.* **2014**, *16*, 14479−14488. (b) Perdew, J. P.; Furche, F. *J. Chem. Phys.* **2006**, *124*, 044103.